

國立臺灣大學電機資訊學院生醫電子與資訊學研究所
碩士論文

Graduate Institute of Biomedical Electronics and Bioinformatics
College of Electrical Engineering and Computer Science
National Taiwan University
Master Thesis

具雙重力學刺激之細胞移動研究微流道裝置
Microfluidic Device with Dual Mechanical Cues for Cell
Migration Investigation



蔡錦雄

Chin-Hsiung Tsai

指導教授：郭柏齡 博士

林致廷 博士

Advisor: Po-Ling Kuo, Ph.D.

Chih-Ting Lin, Ph.D.

中華民國 101 年 7 月

July, 2012

致謝

非常感謝郭柏齡老師和林致廷老師，在這兩年的共同指導，提供許多寶貴的建議，奠基我在學術研究上的基礎。特別感謝郭老師給予我參加學術會議的機會，得以與其他研究團隊交流互動，拓展視野。

雖然同時參加兩位老師的會議、報告以及實驗會較為忙碌，但學術上的收穫卻遠大於付出；而與兩邊實驗室成員日常生活的互動、研究上的討論砥礪，更是令人難忘。特別感謝智傑、毛毛、小田田、Pinky、翊倫提供的協助與歡樂。

謝謝我的父母與姊姊，給予我各種協助，使我得以無後顧之憂，盡力學習。最後要感謝的是與我交往八年的女友高秀華，接受我的優點與缺點，陪伴我走過人生的痛苦與歡笑。

摘要

細胞移動在許多生理現象及疾病扮演非常重要的角色，例如血管新生、傷口癒合以及癌症轉移。因此研究細胞移動的基本機制，將對疾病治療與再生醫學的發展至為關鍵。部分生物力學刺激對細胞移動的影響，已被廣泛研究並深入探討；然而，在多重訊號同時刺激下，細胞將如何受到調控，仍是目前了解甚少的領域。在本篇研究中，我們將具有硬度梯度的水膠整合進入微流道系統中，此一整合型裝置將能同時提供雙重力學刺激去調控細胞移動。藉由此一裝置，我們將能在一個更接近人體生理狀況的環境中，深入探討硬度梯度與滲透壓梯度對細胞移動的影響，此一裝置同時也具有應用在其它研究目的的潛力。

關鍵字：細胞移動、微流道、水膠、硬度梯度、滲透壓梯度

Abstract

Cell migration plays an important role in both physiology and disease, such as angiogenesis, wound healing and cancer metastasis. Therefore, understanding the fundamental mechanisms of cell migration is crucial to create strategies for disease treatment and regenerative medicine. Some biomechanical cues have been well studied about their effects on guiding cell migration, however, few discuss about simultaneously generating dual or multiple cues to affect cell migration. Here, we integrated a gradient-compliant polyacrylamide (PA) gel into the microfluidic system, thus enabling the device to provide dual mechanical cues at the same time. By adopting this advanced device, we can investigate the effects of stiffness and osmotic gradients on guiding cell migration in a more in vivo-like environment, and this dual cues system might also be useful for other applications.

Key words: cell migration, microfluidics, hydrogel, stiffness gradient, osmotic gradient

Content

| | |
|---|-----------|
| 致謝..... | i |
| 摘要..... | ii |
| Abstract | iii |
| Content | iv |
| List of Figures..... | v |
| List of Tables | vi |
| Chapter 1. Introduction..... | 1 |
| Chapter 2. Materials and Methods..... | 6 |
| 2.1 Device design and operation principle | 6 |
| 2.2 Fabrication of microfluidic system | 10 |
| 2.2.1 Photolithography | 10 |
| 2.2.2 Soft lithography | 12 |
| 2.3 Gradient-compliant polyacrylamide gel..... | 13 |
| 2.3.1 Polymerization of the polyacrylamide gel..... | 13 |
| 2.3.2 Functionalization of the polyacrylamide gel | 14 |
| 2.3.3 Characterization of the polyacrylamide gel..... | 15 |
| 2.4 Fabrication and characterization of the dual mechanical cues device | 16 |
| 2.4.1 Fabrication of PDMS substrate..... | 16 |
| 2.4.2 Integration of the PA gel and the microfluidic channels..... | 17 |
| 2.4.3 Quantification of the concentration gradient | 20 |
| 2.5 Osmotic gradients simulation..... | 20 |
| 2.6 Cell culture and cell migration analysis | 22 |
| Chapter 3. Results and Discussion..... | 24 |
| 3.1 The integrated PA gel-microfluidic device | 24 |
| 3.2 Concentration gradients generation and analysis | 27 |

| | |
|---|-----------|
| 3.2.1 Simulation of the sucrose concentration gradient..... | 27 |
| 3.2.2 Trypan blue concentration gradient..... | 30 |
| 3.3 Characterization of the gradient-compliant PA gel..... | 31 |
| 3.3.1 Stiffness gradient | 31 |
| 3.4 C2C12 cell culture and analysis | 34 |
| 3.4.1 Cell culture in the integrated PA gel-microfluidic device..... | 34 |
| 3.4.2 Cell culture in the high osmolarity cell culture medium | 36 |
| 3.4.3 Cell migration on a gradient-compliant PA gel..... | 39 |
| 3.5 Evaluation of 2D and 3D hydrogel-microfluidic integration systems | 42 |
| Chapter 4. Conclusion and Future works..... | 44 |
| Reference | 46 |

List of Figures

| | |
|---|----|
| Fig. 2.1: Schematic of the dual mechanical cues device | 7 |
| Fig. 2.2: Schematic of device operation, dual gradients and signals sensed by the cell..... | 9 |
| Fig. 2.3: Fabrication process of master mold | 11 |
| Fig. 2.4: Fabrication process of PDMS replica | 12 |
| Fig. 2.5: Polymerization of PA gel | 14 |
| Fig. 2.6: Protein conjugation with PA gel..... | 15 |
| Fig. 2.7: Planarization of PDMS substrate | 17 |
| Fig. 2.8: Fabrication process for integrating microfluidic system with PA gel..... | 19 |
| Fig. 3.1: A photograph of the assembled device and the mask design of the microfluidic channels..... | 25 |
| Fig. 3.2: Top-view phase contrast images of the cell culture chamber in the device | 26 |
| Fig. 3.3: Simulation of concentration gradient and data plots..... | 29 |
| Fig. 3.4: A photograph of the trypan blue concentration gradient generated by the device | 31 |
| Fig. 3.5: Stiffness measurement of the gradient-compliant PA gels..... | 33 |
| Fig. 3.6: Fibronectin densities of the PA gels | 34 |

Fig. 3.7: Cell culture after seeding for 24 hours in the devices.....36

Fig. 3.8: Cell culture with or without high concentration sucrose37

Fig. 3.9: Quantitative analysis of C2C12 cell morphology changes under hypertonic stress.....38

Fig. 3.10: Windrose plot of cell migration path and positions of cell tracking on a gradient-compliant PA gel.40

Fig. 3.11: Quantitative analysis of C2C12 cell migration speed and TI.....40

Fig. 3.12: Distribution of cell numbers along a gradient-compliant PA gel.41

List of Tables

Table 1: Quantitative description of C2C12 cell morphology under different hypertonic stress.....38

Table 2: Quantitative description of C2C12 cell migration speed and TI...40

Table 3: A comparison table of 2D and 3D hydrogel-microfluidic integrated systems43

Chapter 1. Introduction

Cell migration plays an important role in physiology and disease (Gardel, Schneider et al. 2010). Cells fail to migrate to the right position during embryogenesis may cause severe development disorders. Cancer cells might change the extra cellular matrix (ECM) and induce a series of events to help them migrate to other organs, the metastasis. For tissue engineering, constructing an appropriate microenvironment and guiding the cells to the right place are critical for cells to function as they did in the original organs. Therefore, understanding the fundamental mechanisms of cell migration is crucial to create strategies for disease treatment and regenerative medicine.

Biochemical and biomechanical cues are two major stimulation types to guide cell migration, and clarifying how these signals affect cell migration is an important research field. Microfluidic systems are capable to generate stable linear or logarithmic chemical gradients and therefore are widely used to study chemotaxis, which describe how chemical factors attract or repel cell migrate along the direction of chemical gradient. Human neutrophils migrate to the place with the highest concentration of interleukin-8 (IL-8) and demonstrate different behaviors to different gradient patterns (Li Jeon, Baskaran et al. 2002). Venular and arterial endothelial cells

show different reactions to the gradient of fibroblast growth factor 2 (FGF2) and different gradient strengths of vascular endothelial growth factor A 165 (VEGFA165) could induce human umbilical vein endothelial cells (HUVECs) to generate different chemotaxis responses (Barkefors, Le Jan et al. 2008).

Astrocyte has been observed to migrate toward hypotonic region under an osmotic gradient (Saadoun, Papadopoulos et al. 2005), and that observation might be involved with the water flow through aquaporins (AQPs) on the cell membrane (Papadopoulos, Saadoun et al. 2008) Some other experiments also show that the osmolarity play a role in controlling cell motility (Loitto, Karlsson et al. 2009). A theoretical study proposes that the osmotic gradient can induce water flux to facilitate the cell motility (Jaeger, Carin et al. 1999). Although the mechanism is still not clear, the osmotic gradient might be a fundamental mechanical stimulation to guide cell migration.

Substrate stiffness is another important mechanical stimulation that has been shown to control the differentiation of mesenchymal stem cells (Engler, Sen et al. 2006) and cell migration. 3T3 fibroblast (Lo, Wang et al. 2000), vascular smooth muscle cells (Wong, Velasco et al. 2003; Isenberg, DiMilla et al. 2009) and macrophages (Nemir, Hayenga et al. 2010) have been demonstrated that they would migrate to stiffer region from softer region of the substrata. This phenomenon is

durotaxis, and the most common material to study how cell response to substrata biophysical signals is polyacrylamide (PA) gel (Gribova, Crouzier et al. 2011). The preparation and characteristics of polyacrylamide gel are well established and studied (Tse and Engler 2010).

Although these studies have shown deep insights to explain the relation between one specific signal and cell migration, there are still few have built an environment providing dual or multiple gradient cues simultaneously. Understanding the cell behaviors under a more *in vivo*-like situation will further extend our knowledge to cell migration and have more reliable information for medical application. However, this idea is mainly limited by the nature that one method can usually generate only one well-controlled signal. One of the approaches to overcome this challenge with microfluidics is designing a functional channel-geometry to generate shear stress gradients in one cell culture chamber, thus it can cooperate with chemical gradient to guide cell migration at the same time (Park, Yoo et al. 2009). Despite their many benefits, there are a number of small, but important, problems. For example, the two stimulations could not be controlled independently since the chemical gradient is also influenced by the flow profile. Another weakness is that the real flow velocity is very difficult to be measured for the flow direction is not simply straight. Moreover, the properties of substrata still could not be changed while these signals are also critical to

guide cell migration.

In this study, we propose a new approach that integrates two different systems into a dual cues device which can generate substrate stiffness and osmotic gradients simultaneously. The two systems in this device are: (1) a gradient-compliant PA gel which is responsible for the first mechanical cue, the substrate stiffness gradient, and (2) a microfluidic system which can generate the second mechanical cue, the osmotic gradient. Sucrose is selected here to adjust the osmolarity of the cell culture media, and it has been used before to study the effect of hypertonic stress on C2C12 cells (Alfieri, Bonelli et al. 2006). The design of the microfluidic system can be divided into two sides: (1) the source side which continues to provide cell culture media with highest sucrose concentration to the cell culture chamber in the microfluidics, and (2) the free side which allows the cell culture chamber to access the bulk solution without sucrose. The gradient is built through the diffusion of sucrose from source side to free side and can be maintained for long term cell culture studies. To develop our dual cues device, we have created two new steps to embed the PA gel in the microfluidic system and protect the gel from damages during the conventional poly(dimethylsiloxane) (PDMS) microfluidics fabrication process.

The C2C12 mouse myoblast is an appropriate candidate to be investigated with osmotic and stiffness gradients. This cell line has been shown that the expression of

AOP5 is regulated by differentiation and hypertonic stress (Hwang, Lee et al. 2002).

The morphology of C2C12 cells is found to depend on substrate stiffness (Engler, Griffin et al. 2004). However, the effects of these mechanical cues on C2C12 cell migration are still not clear.

We hypothesize that C2C12 cell migration can be influenced by both stiffness and osmotic gradients and the two signals can facilitate with each other to guide cell migration. So far, we have successfully performed C2C12 cell culture in our device.

We also cultured C2C12 cells with a high osmolarity cell culture medium in the culture dish, and analyzed cell migration on a gradient-compliant PA gel. These results provide important information for further experiments to test our hypotheses.

The device presented in this study might be the first one to embed a gradient-compliant PA gel in a microfluidic system, and this device has the potential to be used to study cell migration under two different stimulations which is more close to the *in vivo* system. The first stimulation is stiffness gradient, and the second one can be osmotic gradients or theoretically, chemical gradients if the solute is replaced with chemoattractants, thus making the device more flexible to be adopted for other studies.

Chapter 2. Materials and Methods

2.1 Device design and operation principle

The main components of the device are shown in Fig 2.1, a. The microfluidic channel includes the main channels and inlet channels (Fig 2.1, b), and their main function is to provide fresh cell culture medium, remove the waste produced by the cells and generate osmotic gradients. Polyacrylamide (PA) gel is used to provide stiffness gradient. The Glas_1 is used to hold PA gel and overcome the challenge that PA prepolymer solution is difficult to polymerize on PDMS. The square groove on PDMS substrate is for Glass_1 and PA gel to be embedded in. The main function of Glass_2 is holding PDMS substrate to ensure the surface of groove on PDMS substrate is smooth, it's more important for thin PDMS substrate (i.e. less than 600 μm). The inlet is connected with a syringe pump, and the outlet is a one side of the main channel (Fig 2.1, c). The important dimension of each component is shown in Fig 2.1, d.

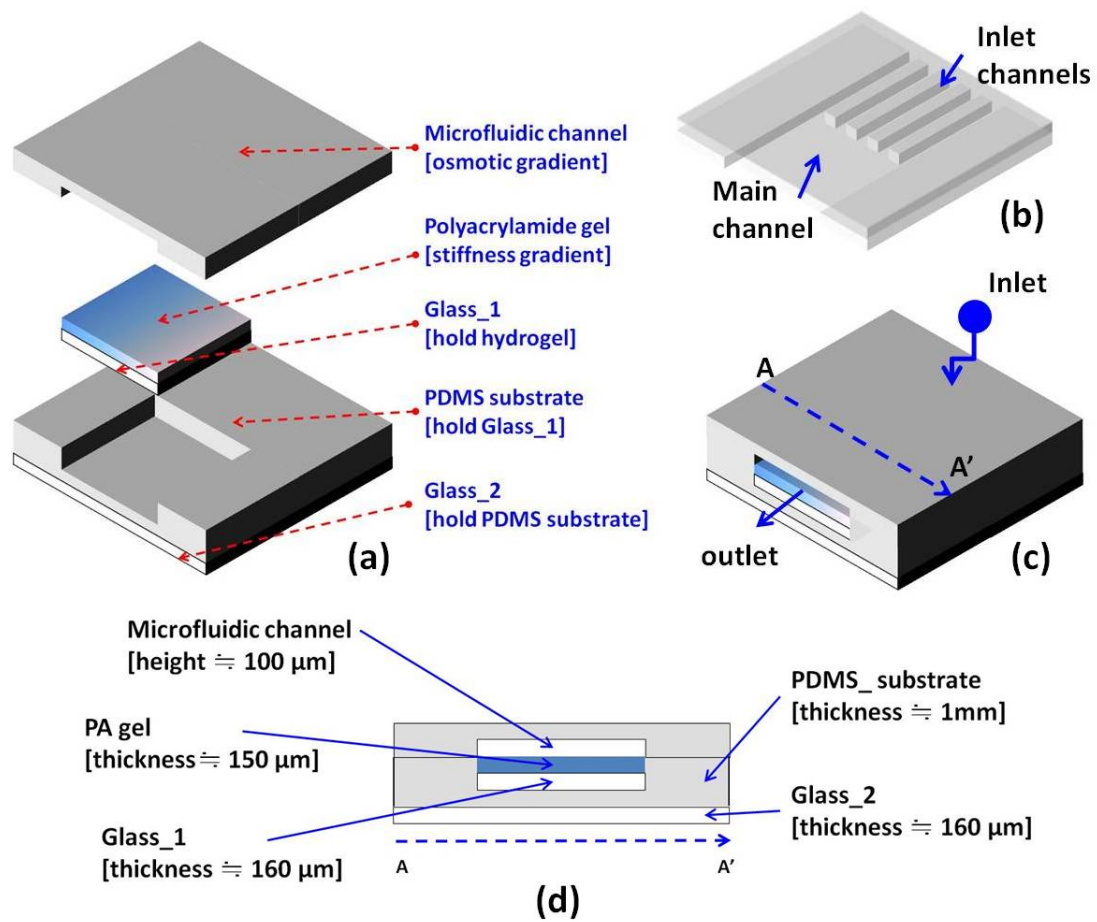


Fig. 2.1: Schematic of the dual mechanical cues device (not to scale). (a) Main components and their functions (in square bracket) of the device. (b) Perspective view of the top layer, the inlet channels and the main channel. (c) Positions of inlet and outlet, the blue circle represents the syringe pump. (d) Cross section view of the A to A' line in (c).

The operation principle of the dual mechanical cues device is illustrated in Fig 2.2. The region where inlet channels connected to the main channel is the source side for high osmolarity cell culture media (high concentration of sucrose), and the outlet of the main channel is connected to the bulk solution where is sucrose-free cell culture media (Fig 2.1, a and Fig 2.2, a). Because the flow velocity driven by the syringe pump is small ($\approx 1 \times 10^{-9}$ m/sec) in the main channel, the distribution of sucrose would be similar with the result from diffusion, thus creating a concentration gradient in the direction from inlet to outlet. The cell migration experiment is performed in the cell culture chamber composed of the main channel and a compliant-gradient PA gel. The direction of the two stimulations, stiffness and osmotic gradients, in the cell culture chamber is shown in Fig 2.2, b, and they are perpendicular with each other. However, it is flexible to change the relative direction between them dependent on the requirement of different experiments. Fig 2.2, c shows the concept about how the two signals simultaneously stimulate a cell in the cell culture chamber. The cell can not only sense the osmolarity difference between the front and the back, but also stiffness difference between the left side and the right side of the cell.

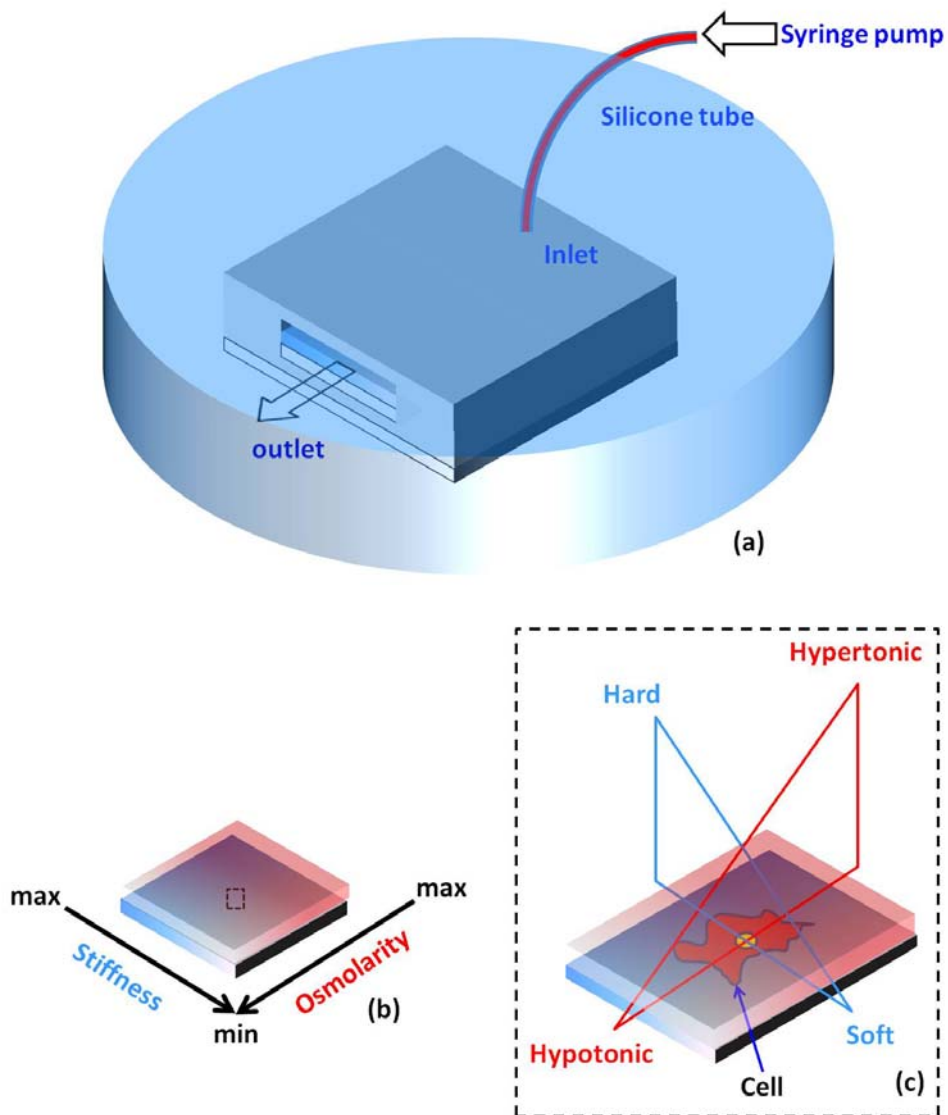


Fig. 2.2: Schematic of device operation, dual gradients and signals sensed by the cell (not to scale). (a) The whole device, except the inlet tube, is immersed in the standard cell culture media. (b) The color changes indicate the intensity distribution from maximum to minimum of the two stimulations in the cell culture chamber. (c) Enlarged dashed-line box in the middle of (b) shows the two different gradient signals sensed by the cell attached on the PA gel.

2.2 Fabrication of microfluidic system

2.2.1 Photolithography

The microfluidic channels (Fig 2.1, a) was fabricated by soft lithography. The first step was to build the master mold by photolithography (Fig 2.3). We used silicon wafer as the substrate for photoresist (PR), SU8-2050. The wafer was cleaned with buffered oxide etch (BOE) to remove the native oxide to promote the adhesion of PR on the substrate (Fig 2.3, a). The PR (shown in yellow in Fig 2.3) was poured on the wafer and spin at 1600 rpm to have a thin-film with thickness of 100 μm (Fig 2.3, b). After the spin coating process, bake PR at 65°C for 5 minutes then 95°C for 20 minutes on a hotplate and finally leave PR to cool to room temperature (Fig 2.3, c). Right after soft bake, use UV light to expose the PR under a photomask to transfer the pattern from the mask to PR (Fig 2.3, d). The energy used in the exposure process is 7 mJ/cm^2 and the exposure time is 35 sec. Then replace the wafer to the hotplate for post exposure bake process, bake the PR at 65°C for 5 minutes then 95°C for 10 minutes and finally leave PR to cool to room temperature. The shape of patterns should appear after the baking process (Fig 2.3, e). After post exposure bake, immerse PR in the Microchem's SU-8 developer, and develop PR for 7 minutes (or until the non-pattern PR is removed) with an ultrasonic bath (Fig 2.3, f). Then rinse the PR

with fresh developer solution, isopropyl alcohol (IPA) and deionized water sequentially. Air dry with nitrogen, then bake the PR at 150°C for 2 minutes (Fig 2.3, g). Silanize the product with dichlorodimethylsilane (DCDMS) in a desiccator overnight to form a thin film on PR and wafer (red film in Fig 2.3, h). That film could prevent PR from damage during fabricating PDMS replica. After these processes, we had a silanized master mold of the microfluidic channels.

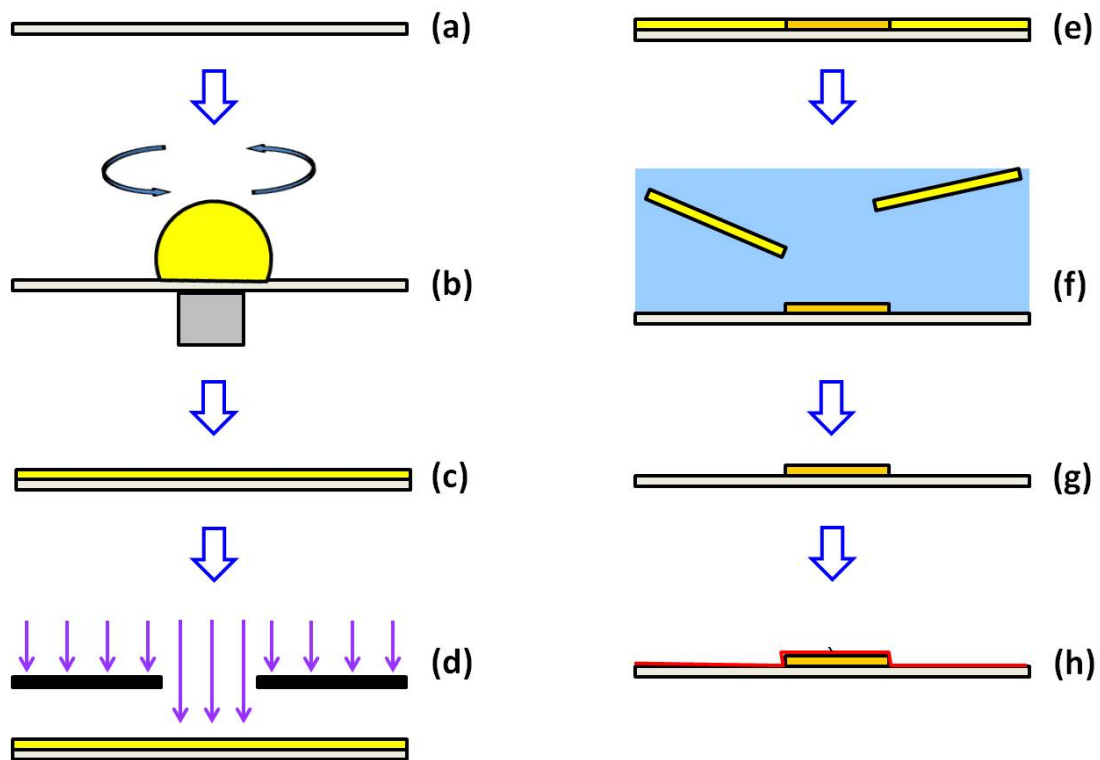


Fig. 2.3: Fabrication process of master mold. (a) Clean the surface of the silicon wafer. (b) Spin coat the SU8-2050 PR (yellow drop) on the silicon wafer. (c) Soft bake. (d) Exposure PR. (e) Post exposure bake. (f) Develop. (g) Hard bake. (h) Silanize the SU-8 precursor.

2.2.2 Soft lithography

The second step of soft lithography is shown in Fig 2.4. Pour Sylgard 184 (PDMS prepolymer: curing agent in 10:1 by weight) on the master mold and cure it at 60°C for at least two hours (Fig 2.4, a). Remove the PDMS replica from master mold (Fig 2.4, b) and punch a hole on the replica for inlet, then autoclave it at 120°C for 30 minutes (Fig2.4, c) to promote the polymerization of PDMS and decrease uncrosslinked oligomers, which might be toxic to cells (Hanson, Cui et al. 2011). The PDMS replica or microfluidic channels were ready to be used in the integration process (Fig 2.8, c).

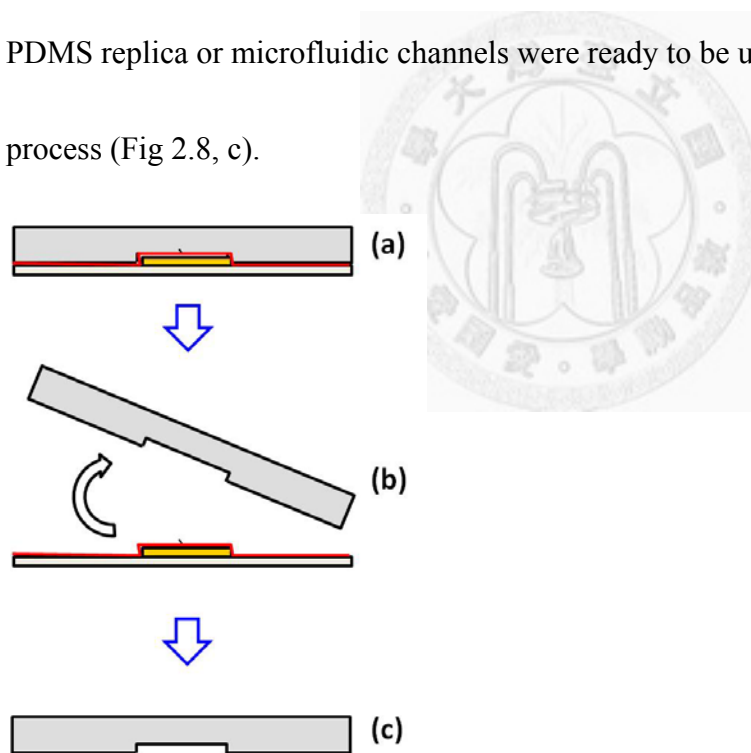


Fig. 2.4: Fabrication process of PDMS replica. (a) Pour the mixture of PDMS prepolymer and curing agent (10:1 by weight) on the silanized master mold, then cure it at 60°C. (b) Replace the PDMS replica from the master mold. (c) Punch a hole for inlet, then autoclave the PDMS replica for 15 min.

2.3 Gradient-compliant polyacrylamide gel

2.3.1 Polymerization of the polyacrylamide gel

The preparation of gradient-compliant PA gel is slightly modified from Engler's protocol (Tse and Engler 2010). Briefly, the PA prepolymer solution was polymerized between two coverslips (Fig 2.5). One of the coverslip was modified with glutaraldehyde to enhance PA gel to attach on coverslip, and this modification is especially important for gradient-polymerized PA gel. The other coverslip was modified with dichlorodimethylsilane (DCDMS) to make the surface hydrophobic to smooth the surface of the PA gel. The PA prepolymer solution was composed of 10% acrylamide (w/v ratio), 0.3% bis-acrylamide, 0.4% acrylic acid, 0.5% Irgacure 2959 (photoinitiator) and deionized water. The intensity of the stiffness gradient can be controlled through exposure time, mask opacity, the concentration of Irgacure 2959 and UV power.

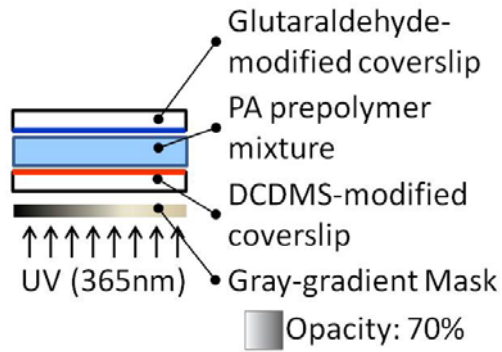


Fig. 2.5: Polymerization of PA gel. The PA prepolymer solution sits in between GA activated coverslip and DCDMS activated coverslip, then polymerize the prepolymer solution with UV light (wavelength = 365nm) filtered with a photomask, thus generating a non-uniform polymerization in the PA prepolymer solution.

2.3.2 Functionalization of the polyacrylamide gel

The PA gel could be further modified to functionalize the surface with extra cellular matrix proteins, for example, fibronectin (Fig 2.6). The method of protein conjugation was through carbodiimide-mediated cross-linking (Kadow, Georges et al. 2007). However, we used 1-(3-(dimethylamino) propyl)-3-ethyl-carbodimide methiodide (ETC) instead of 1-ethyl-3-(3-dimethylaminopropyl) carbodiimide hydrochloride (EDC). Because the molecular weight between ETC and EDC is different, from our experience, the appropriate concentration of ETC is 40.3 mg/ml. The concentration of fibronectin is 100 μ g/ml.

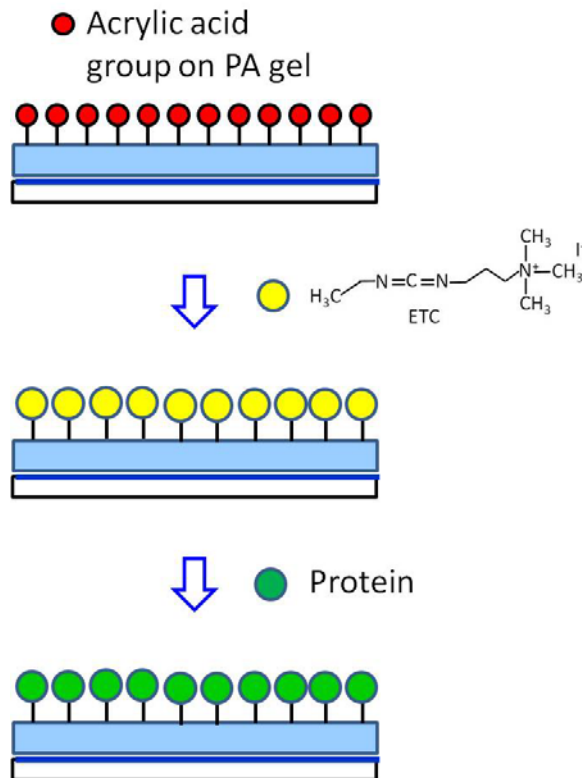


Fig. 2.6: Protein conjugation with PA gel. The ETC (yellow) can react with acrylic acid (red) of PA gel to form an unstable intermediate, which can react with the protein (green), thus conjugating the protein on the PA gel.

2.3.3 Characterization of the polyacrylamide gel

We used immunofluorescence to verify a uniform density of fibronectin conjugation among the gradient-compliant PA gel. The primary antibody (anti-fibronectin) was diluted with PBS (4% BSA) in 1:400, and the secondary antibody (anti-rabbit) was diluted with PBS (4% BSA) in 1:600. The fluorescent images were analyzed by Image J.

The measurement of PA gel stiffness was kindly assisted by Bioceramics and

Composites Lab in institute of biomedical engineering, national Taiwan university.

We used TR800PB probe with spring constant about 0.615 N/m to 0.731 N/m, and the

Possion ratio of PA gel was defined as 0.42 (Engler, Rehfeldt et al. 2007).

2.4 Fabrication and characterization of the dual mechanical cues device

2.4.1 Fabrication of PDMS substrate

Besides the microfluidic channels, we also used soft lithography to make another PDMS replica, the PDMS substrate for holding Glass_1 (Fig 2.1, a). The process is shown in Fig 2.7. We used laser ablation to trim a transparency film to a square (5.1 mm x 5.1 mm), then attached it on the glass with 3M double tape. It is the master mold for the groove in the PDMS substrate. Poly (methyl methacrylate) (PMMA) was used here as a spacing to define the thickness of PDMS substrate. PDMS prepolymer solution was poured on the master mold, then we placed a DCDMS modified glass dish on the PMMA. The extra PDMS solution was squeezed out by applying a force on the glass, then the whole setup was placed in an oven to cure the PDMS. This smoothing process enables the surface of groove on the PDMS to be flat after bonding to Glass_2, thus increasing the success rate of bonding between Glass_1 and PDMS substrate.

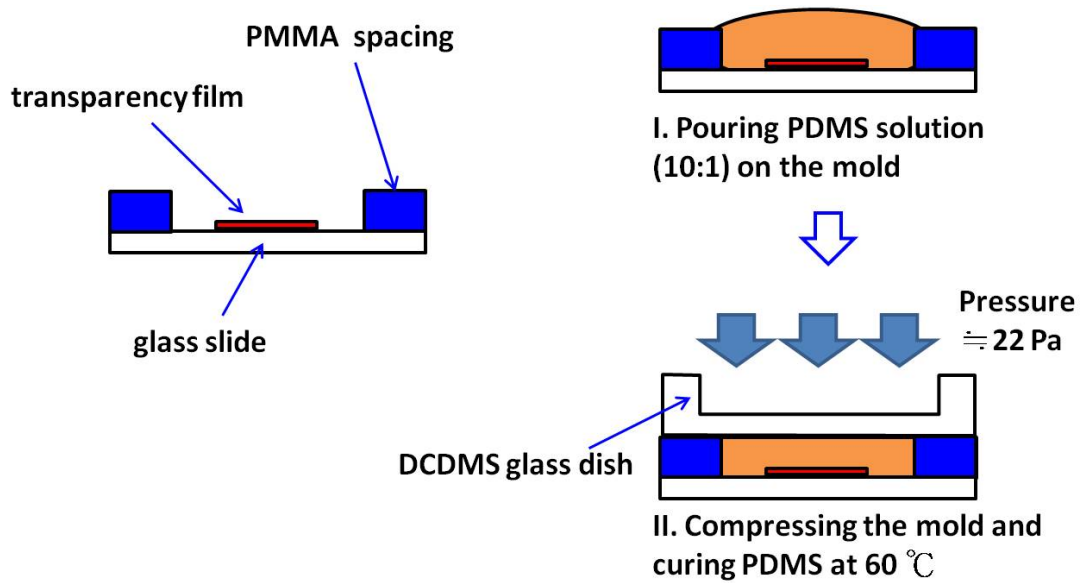


Fig. 2.7: Planarization of PDMS substrate. The master mold of PDMS substrate is fabricated by attaching customized PMMA spacing and transparency film with 3M double tape to the glass slide. Then use standard PDMS replication process and pressurized glass dish to smooth top surface of the PDMS replica.

2.4.2 Integration of the PA gel and the microfluidic channels

The integration process of the PA gel and the microfluidic system (Fig 2.8) started from assembling Glass_1, PDMS substrate and Glass_2. We used oxygen plasma bonding method and it would render the PDMS surface to be hydrophilic. Therefore, we had to cover the non-bonding area with 3M tape to retain their hydrophobicity, which prevented chemical solutions spreading from the groove during the surface modification process of Glass_1. The PA polymerization process was

similar with the description in section 2.3.1. During this process, the extra silane on the DCDMS-modified coverslip had to be removed, or it would transfer to the PDMS surface and make these areas unable to be activated by air plasma. The final bonding process (Fig 2.8, c) was completed as fast as possible to decrease the possibility to dehydrate the PA gel, and we also use a customized coverslip (5 mm x 5mm) to protect the PA gel from reactive ion species. The fastest bonding condition (18W, 890 mtorr, 33 sec) we had was achieved through performing the air plasma activation under higher process pressure. The device was filled with deionized water to prevent the PA gel from dehydration, some bubbles might appear during this process. After sterilizing the device with UV light, we immersed it in deionized water overnight to remove bubbles, then injected the ETC solution through the inlet to perform the protein-PA gel conjugation process (section 2.3.2). The functionalized device was ready to be used in cell culture experiments or kept in PBS at 4°C.

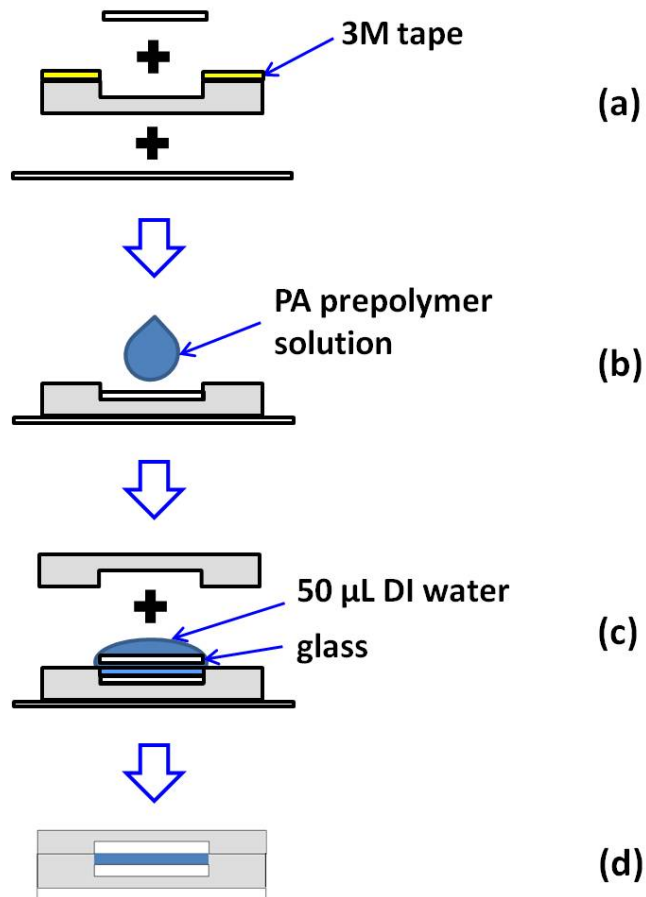


Fig. 2.8: Fabrication process for integrating microfluidic system with PA gel.

(a) Use oxygen plasma to activate Glass_1, PDMS substrate and Glass_2 except non-groove area of the PDMS substrate (protected by 3M tape). Bond PDMS substrate and Glass_2 first, and then bond Glass_1 to the surface of the groove. After completing the bonding process, re-activate Glass_1 with oxygen plasma again. (b) Modify the Glass_1 surface and then polymerize the PA prepolymer solution on the glass. (c) Treat the microfluidic channel and the product from step (c) with air plasma except the PA gel area, and bond them together. (d) Leave the device at room temperature for at least 30 minute to enhance the bonding effect.

2.4.3 Quantification of the concentration gradient

We used trypan blue ($M_w = 872.88$ Da) as the solute to observe the color gradient to simulate the sucrose ($M_w = 342.3$ Da) gradient in the cell culture chamber. We captured the images continuously from A to A' (Fig 3.4) with a phase contrast microscope. The gray intensity of each image was analyzed by Image J. We defined the average intensity of the final 100 points as the background (I_B). The gray intensity of each data point (except the final 100 points) subtracted from I_B to I_C . The minimum of I_C was defined as I_M , and the normalized concentration of each point was defined as:

$$\text{Normalized concentration} = \frac{I_C}{I_M}$$

2.5 Osmotic gradients simulation

In our study, we used sucrose to control osmolarity, thus the osmolarity difference sensed by a cell is proportional to the concentration gradient of sucrose. To predict the concentration gradient and the flow velocity profile in the cell culture chamber (Fig 2.2), we used COMSOL Multiphysics 4.2a to simulate these distributions in a two-dimensional simulation. In the two simulations below, the fluid was defined as incompressible flow and neglect inertial term. The diffusion coefficient of sucrose was defined as 5×10^{-10} m²/s for free flow media. All the results

were presented in the equilibrium state except the concentration-time dependent change (Fig 3.3, b).

For the top view to the cell culture chamber, we coupled two physical models, laminar flow and transport of diluted species, to perform the sucrose concentration and flow profile in the free flow area. The normal inflow velocity was 1×10^{-7} m/s, the inflow concentration was 200 mM, and the outflow concentration was 0 mM since we assumed that the solutes disappeared quickly as they accessed to the bulk area.

The mesh settings was physics-controlled mesh consisted of 2012 elements (normal).

The characteristics of water were generated from the default setting in COMSOL Multiphysics.

For a more specific simulation to our device, we used the other two physical models, Brinkman equations and species transport in porous media. This model construction could give us a more realistic prediction since the substrate in the cell culture media was PA gel, a porous medium. We built the whole model according to COMSOL model gallery (model ID: 170). In Brinkman equations, the fluid properties were generated from the default setting of water, while the porous matrix properties were user defined. The porosity of porous medium gel was defined as 0.3 between solid (0) and free flow (1), and permeability was defined as 1×10^{-14} m² (Grattoni, Al-Sharji et al. 2001). The porosity of free flow area was defined as 1, and

permeability was defined as 1 m^2 . For setting species transport in porous media, we defined the porosity of PA gel as 0.3, and bulk density 1000 kg/m^3 to represent water. The diffusion coefficient of sucrose in porous media was defined as $1 \times 10^{-10} \text{ m}^2/\text{s}$, which was smaller than that in free flow media. The other parameters were defined as in the previous case, and the mesh settings was physics-controlled mesh consisted of 5125 elements (coarser).

2.6 Cell culture and cell migration analysis

The cell line used in our studies was C2C12 mouse myoblast cells. The cells were kept in the conventional incubator (37°C , $5\%\text{CO}_2$) and supplied with cell culture media (10% FBS and 1% antibiotics in Dulbecco's Modified Eagle's Medium). For cell culture test in the device, the cells were delivered to the cell culture chamber by pipeting the cell suspension (10^6 cells/ml) several times in front of the outlet. When culturing cells in high osmolarity culture media, we added sucrose to increase the osmolarity and had the cell density relatively low (2000 cells/cm^2) to decrease the possibility of cell-cell contact.

For cell migration experiments, the cell density on the PA gel was 1850 cells/cm^2 . The cells were cultured at conventional incubator for 24 hours before cell migration tracking. During the cell migration tracking, the cells were cultured at a customized cell culture chamber on a motor stage of the microscopy. The environment was kept

as in a conventional incubator.

To analyze the cell migration on a gradient-compliant PA gel, we tracked the cells by a phase contrast microscope. Six fields from the hard regions to the soft regions were chosen and captured at 20 min intervals over 8hrs through CCD digital camera. Cells that came into contact with each other were excluded from tracking. We used a Labview program to identify the centroids of the cells, and the data were transferred to the excel format, which can be imported to Image J (chemotaxis_tool) for further analysis. The windrose plots were shown for qualitative results of cell migration path. The tactic index (TI) was used to quantitatively describe how strongly the cell migration was influenced by the stimulation (Isenberg, DiMilla et al. 2009; Sochol, Higa et al. 2011).

$$TI = \frac{X}{L}$$

X: mean displacement along gradient direction; L: total path length

TI would be 0 if the cell migration was unbiased, and 1 if it was fully biased.

After being incubated for 48hrs, cells were fixed and stained with 4',6-diamidino-2-phenylindole dihydrochloride (DAPI) to count the number of cells in different places on the PA gel. All the statistical analyses were performed with *t*-test except one sample *t* test for tactic index.

Chapter 3. Results and Discussion

3.1 The integrated PA gel-microfluidic device

A photograph of our device is shown in Fig 3.1, and a picture of the photomask is also shown below it to demonstrate the microfluidic channel design more clearly. The long inlet channels are designed to increase the hydraulic resistance in these channels, and that high resistance can increase the flow stability in the source side of the cell culture chamber. This will be important to have uniform concentrations along the direction perpendicular to the input flow. The whole device is transparent, which is an advantage for cell-research users because this will be compatible to their daily instrument, for example, the phase contrast microscope. However, the thickness (1 mm) of the PDMS substrate will be an issue if the user wants to study cell organelles or cytoskeletons. The possible solution for the thickness issue will be further discussed in chapter five. Air bubbles appear sometimes in the device during injecting deionized water into the cell culture chamber by connecting the inlet to the syringe. However, it does not affect the performance of the device since the bubbles will disappear easily when we immerse it in the deionized water overnight. The device can be kept in sterilized deionized-water for over one week before the functionalization process of the PA gel.

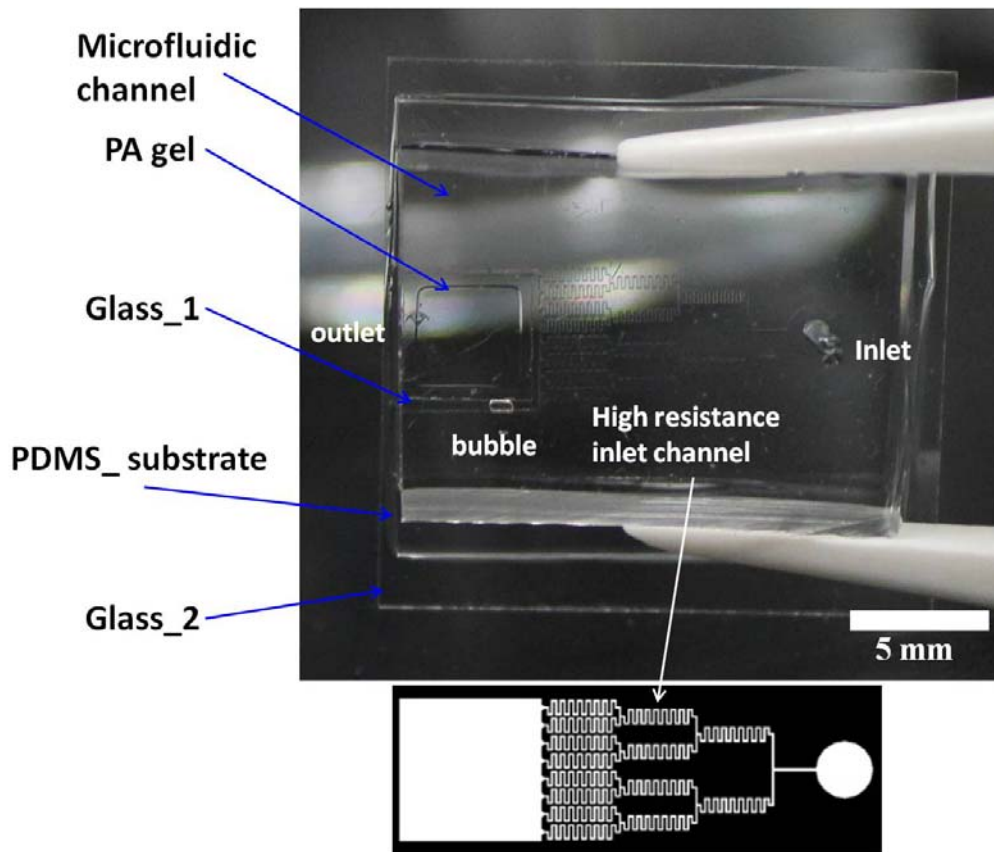


Fig. 3.1: A photograph of the assembled device and the mask design of the microfluidic channels.

Some of the misalignments were shown in Fig 3.2. The possibility of misalignments during bonding process can be largely decreased though designing lock and key structures to the microfluidic channels and the PDMS substrate, respectively. Another misalignment is caused by that the PA gel were not fully cover the Glass_1 (Fig 3.2, c). PDMS might lead to this consequence because it can interfere with the polymerization of PA gel. To our knowledge, there is no appropriate explanation to this phenomenon, thus making this issue much difficult to be solved. Despite of this issue, the device is still capable to generate a stable concentration

gradient when the input flow is slow enough to make the solute can only move through diffusion in the cell culture chamber.

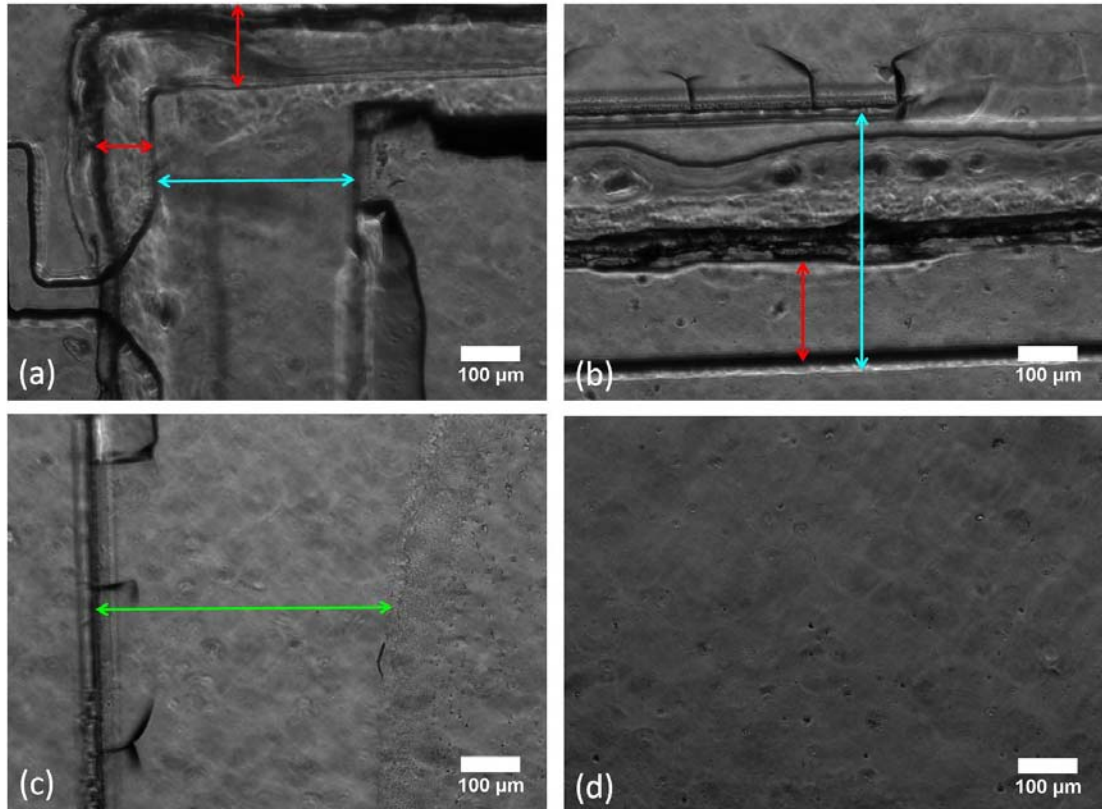


Fig. 3.2: Top-view phase contrast images of the cell culture chamber in the device. (a), (b) and (c) indicate the misalignments of the device. Red arrows mean the distance between the edge of microfluidic channels and the edge of the PDMS substrate. Blue arrows: microfluidic channels and Glass_1. Green arrow: Glass_1 and PA gel. (d) The surface of the PA gel in the device.

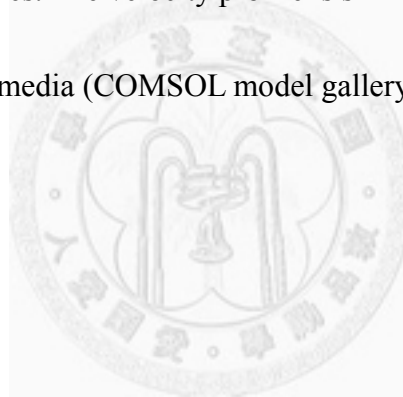
3.2 Concentration gradients generation and analysis

3.2.1 Simulation of the sucrose concentration gradient

The simulation results are shown in Fig 3.3. There are eight inlet ports to the cell culture chamber, and these eight point sources form a line source to supply the solute to diffuse into the cell culture chamber. The line source will be more appropriate to generate uniform concentration gradient along different position of y-axis. The arrow surface also shows the velocity field is uniform in the cell culture chamber. The data suggests that the device needs six to ten hours to have a stable gradient (Fig 3.3, b) by computing the gradients change along the white arrow (Fig 3.3, a) in a time dependent study. From these simulations, we also noted that the highest concentration in the source side of cell culture chamber is slightly lower (e.g. 190 mol/m^3) than the inflow setting (e.g. 200 mol/m^3). In fact, when the position of the inlet was set much far from the cell culture chamber, this concentration drop between the inlet and source side would be more significant (e.g. 200 mol/m^3 to 65 mol/m^3 , data not shown). That can be an important reference to decide what the concentration would be in the inlet to generate the gradients we need in the cell culture chamber.

Considerate the cell culture chamber is constructed from free flow area (the main channel in Fig 2.1, b) and porous media (PA gel), we analyzed the concentration

distribution in the cross section area (Fig 3.3, c). There is no significant difference in the concentration distribution between free flow area and porous media when we set the thickness of the two layers are equal to 100 μm . However, the flow velocity profiles in these two areas are quite different caused by the low permeability (10^{-14} m^2) of the PA gel. The highest flow velocity in the free flow area is about 0.15 $\mu\text{m}/\text{sec}$ (Fig 3.3, d), but it is almost zero in the porous media. It might explain that the fluorophore still existed in the PA gel after wash the whole cell culture chamber with deionized water several times. The velocity profile is similar with other simulation work for free flow-porous media (COMSOL model gallery, Model ID: 170).



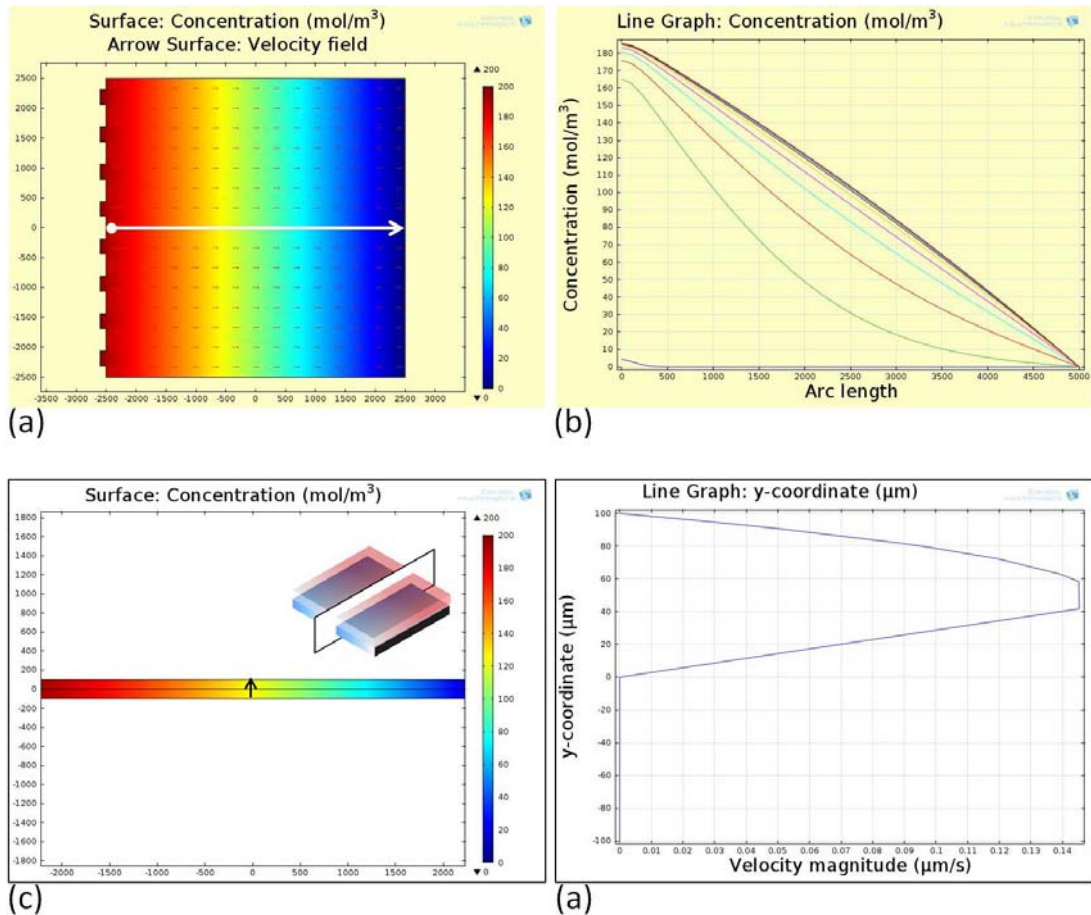


Fig. 3.3: Simulation of concentration gradient and data plots. (a) Top-view of the concentration gradients in the cell culture chamber. (b) A time-dependent change of the concentration gradient along the white arrow in (a). (c) A cross section view of the concentration gradients in the cell culture chamber. (d) Perpendicular velocity profile along the black arrow in (c).

3.2.2 Trypan blue concentration gradient

The concentration gradient of trypan blue generated by our device is shown in Fig 3.4. This color gradient existed for over than 36 hours. The concentration gradient upon the PA gel ($A \rightarrow A'$) is plotted on the right figure. Despite the experimental result dose not fit much to the simulation result, they give the same trend. Besides the structure defects described in section 3.1 (Fig 3.2, a, b and c), the non-well controlled flow rate might also lead to this consequence. The syringe pump can generate flow rate below than $0.1 \mu\text{L/hr}$, which is slow enough to have a concentration gradient in the cell culture chamber from the simulation work. However, we often failed to generate concentration gradients in the real operation. In some fluorescent experiments, the whole bulk area (Fig 2.2, a) emitted fluorescence after operating the device at a flow rate of $0.053 \mu\text{L/hr}$ for 24 hours. The fluorescent intensity of the bulk area was larger than the intensity of the PA gel area. That might be explained by the flow was not slow enough to have a more diffusion-like solute distribution. In the case shown in fig 3.4, we used a passive pump to generate the flow, but the protocol to operate passive pump has not been established. A more sophisticated method to control the flow velocity might be a priority.

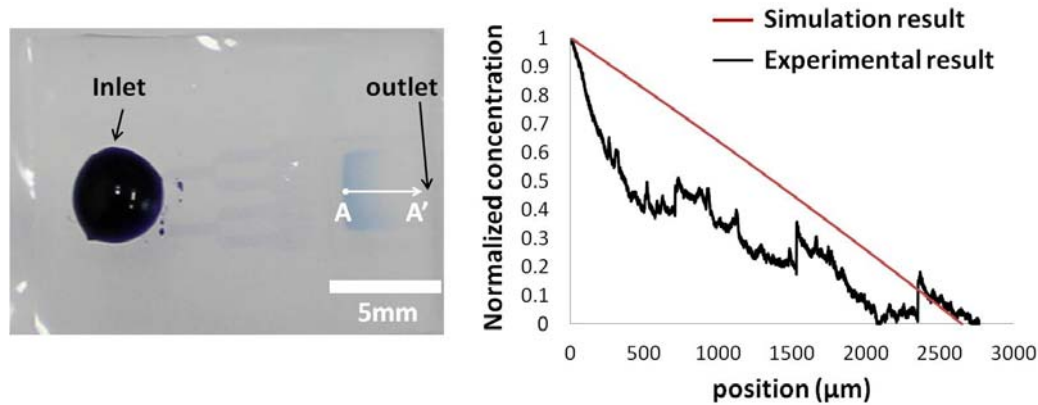


Fig. 3.4: A photograph of the trypan blue concentration gradient generated by the device. The data plot (right) describes the concentration gradient from A to A' (left), which is the width of the PA gel.

3.3 Characterization of the gradient-compliant PA gel

3.3.1 Stiffness gradient

The gels used here were polymerized on a coverslip ($18 \times 18 \text{ mm}^2$), and the only different parameter of these two gels is exposure time: 8 minutes (Fig 3.5, a) and 7.5 minutes (Fig 3.5, b). The data plots suggest that there might be a saturation zone in the hardest region. The measurement of the soft region is difficult to get accurate data. Therefore, the linear stiffness gradient only exists in the middle region (more than one-fourth of the total area). The strength of the gradients (4.43 kPa/mm and 3.51 kPa/mm) should be enough to induce durotaxis for vascular smooth muscle cells (Wong, Velasco et al. 2003). However, it should be careful to apply these data to have a quantitative analysis with regard to the relationship between stiffness gradients and

cell migration. It is difficult to establish an effective protocol to measure the soft material like PA gel with an atomic force microscope. Furthermore, PA gel may not be a purely elastic substrate and some data processing will be necessary to provide more accurate information (Isenberg, DiMilla et al. 2009). Even with this quantitative analysis issue, the gradient polymerization method is still easy and robust to generate gradient-compliant PA gel.



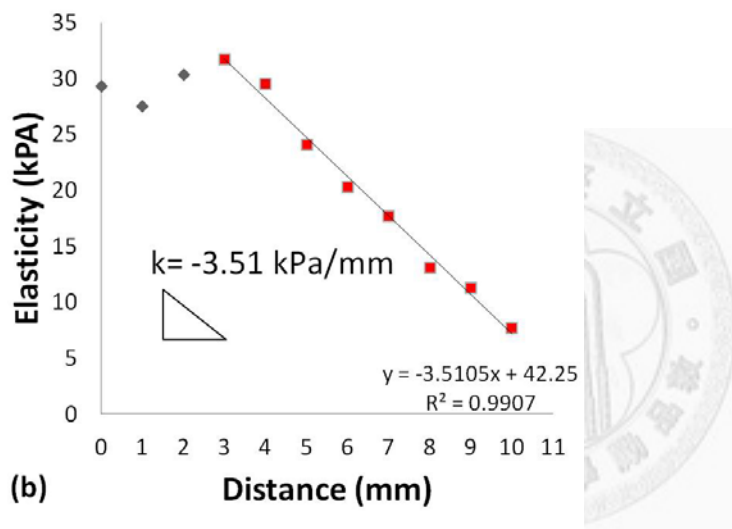
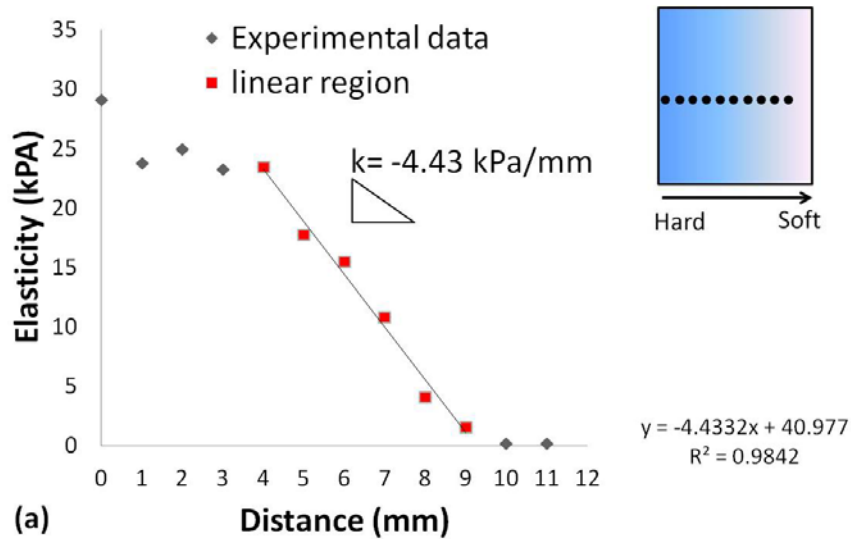


Fig. 3.5: Stiffness measurement of the gradient-compliant PA gels. The distance between two measured points is 1 mm, and the measurement was conducted continuously from the hard region to the soft region. The data is the average elasticity of each point. (a) Exposure time: 8 minutes. (b) Exposure time: 7.5 minutes.

3.3.2 Fibronectin densities

There is no significant difference of the fluorescence among different positions on the gradient-compliant PA gel. For comparison, the uniform-gradient PA gel is also showed. These results suggest that the difference of stiffness or polymerization degree would not affect the protein conjugation to the PA gel. The fluorescent intensity profile is similar with other research (Isenberg, DiMilla et al. 2009).

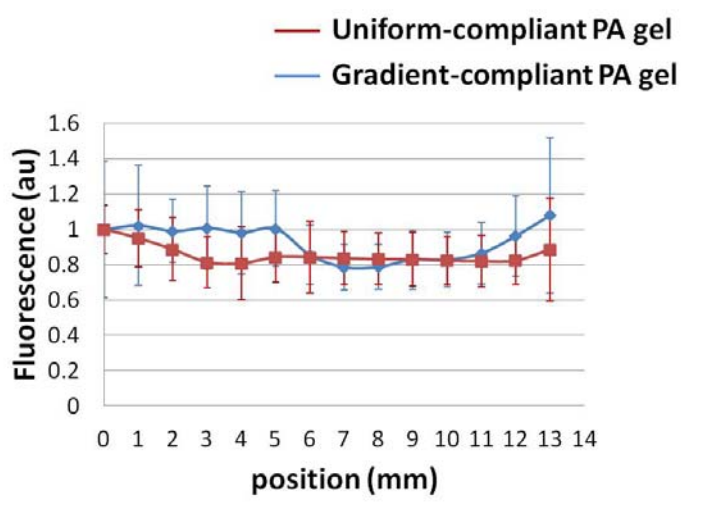


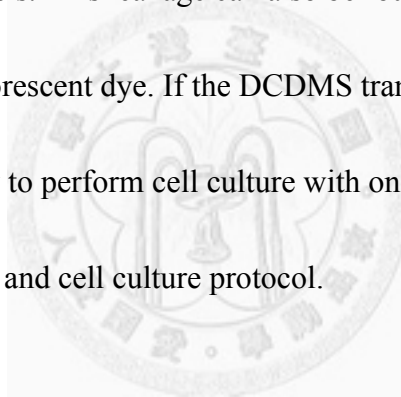
Fig. 3.6: Fibronectin densities of the PA gels. Data are shown in Mean \pm SD.

3.4 C2C12 cell culture and analysis

3.4.1 Cell culture in the integrated PA gel-microfluidic device

We have cultured C2C12 cells in four different devices (Fig 3.7). Three of four are successful, and the one (device 4) failed to culture cells might have a non-functionalized PA gel. This assumption is lead by two observations. First, there are cells attached on Glass_1 in device 4, thus the ECM protein and other conditions

(pH, temperature..etc.) must function appropriately. Second, even the rough surface in device 3 doesn't affect cell culture much. The cause of failed ETC-fibronectin reaction should come from inappropriate bonding between microfluidic channel and PDMS substrate. As mentioned in section 2.4.2, the DCDMS might transfer to the surface of PDMS substrate and make bonding failed in the contaminated area. When injecting the reactants into the failed-bonding device with a syringe, the flow will leak out the device through these failed-bonding regions, which are lower hydraulic resistance channels. This leakage can also be found when the failed-bonding device was tested with fluorescent dye. If the DCDMS transfer issue is addressed properly, the device is easy to perform cell culture with only slightly changes of functionalization of PA gel and cell culture protocol.



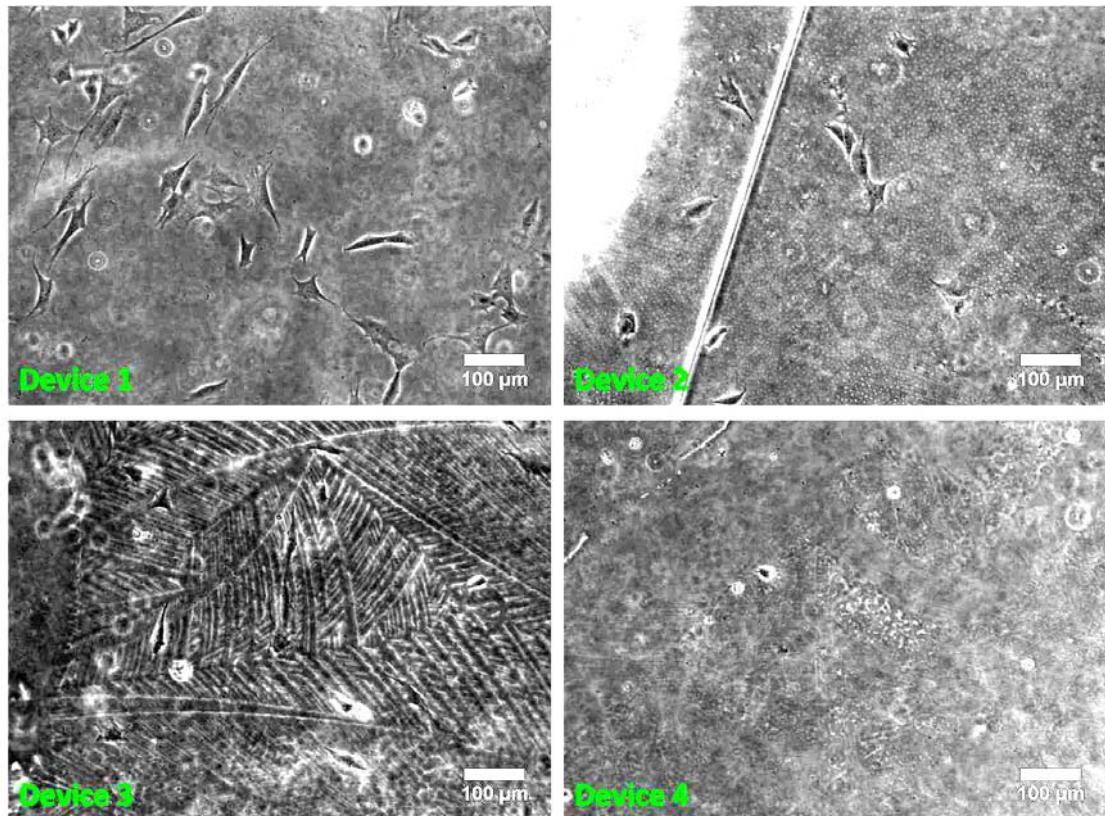


Fig. 3.7: Cell culture after seeding for 24 hours in the devices. Only device 4 failed to have a normal cell culture result.

3.4.2 Cell culture in the high osmolarity cell culture medium

After culturing the C2C12 cells in the conventional culture dish with high osmolarity cell culture medium for 7 hours, most of the cells still did not spread out (Fig 3.8, 200mM). The osmolarity of DEME we used is 332-352 mM/kg, thus the osmolarity of the cell culture medium with high concentration sucrose would be about 532-552 mOsm. The osmolarity more than 500 mOsm may decrease the cell viability (Alfieri, Bonelli et al. 2006). However, some of the cells can spread out after exposing to hypertonic environment for 26 hours, though the average cell area is still smaller

than control group (Fig 3.9). The effect of high osmolarity on cell morphology, projection area, perimeter and circularity ratio, would be much clear by comparing with the results of control group ($p < 0.001$). The findings are different from other studies which show that hypertonic stress didn't induce significant morphological differences of C2C12 cells or even induced an opposite response (Hwang, Lee et al. 2002; Van Donkelaar, Daniels et al. 2003). Non-confluent cell culture or single cell culture might be important for C2C12 to have a different response under hypertonic stress. Moreover, this cell morphology changes between different time periods of hypertonic stimulation may imply C2C12 cells can sense and adapt to the hypertonic environment. Therefore, it is possible that C2C12 cells can respond to an osmotic gradient. A quantitative description of cell morphology is shown in table 1.

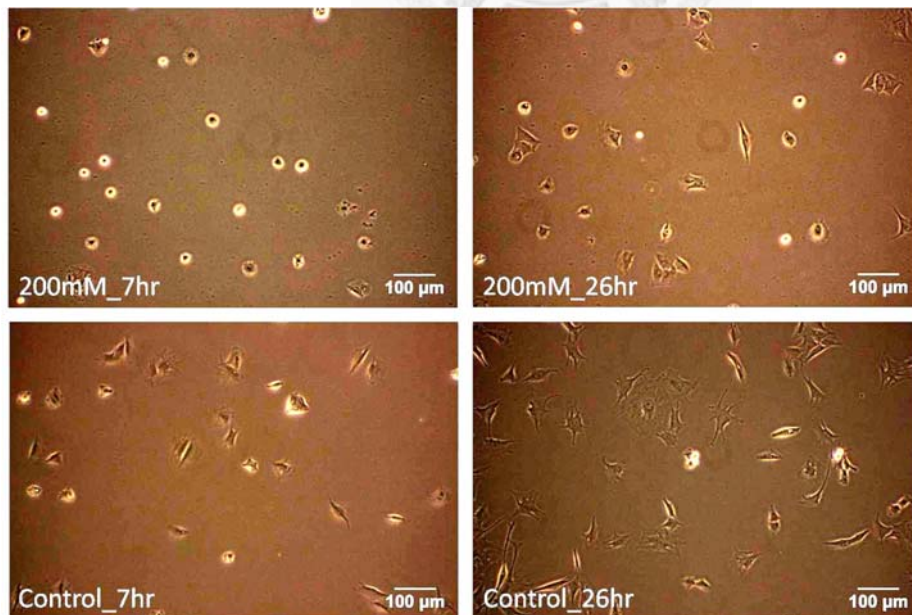


Fig. 3.8: Cell culture with or without high concentration sucrose.

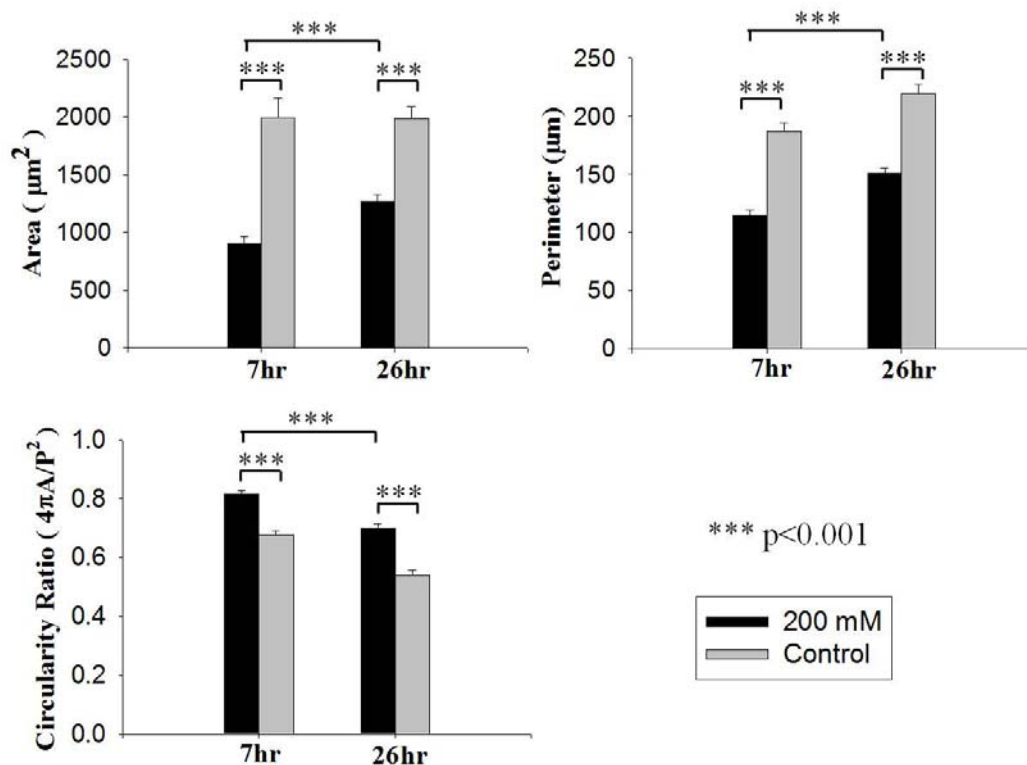


Fig. 3.9: Quantitative analysis of C2C12 cell morphology changes under hypertonic stress. Treat C2C12 cells treated with hypertonic medium significantly induce morphological changes. The morphological differences between experimental groups (7hr and 26hr) imply a compensatory mechanism to the hypertonic stress

| 7 hr | 200 mM (n=71) | Ctrl (n=66) |
|-----------|-----------------|------------------|
| Area | 906.46 ± 60.63 | 1994.81 ± 172.49 |
| Perimeter | 115.12 ± 4.17 | 187.14 ± 7.48 |
| C.R. | 0.82 ± 0.01 | 0.68 ± 0.02 |
| 26 hr | 200 mM (n=87) | Ctrl (n=104) |
| Area | 1270.10 ± 58.52 | 1985.46 ± 101.91 |
| Perimeter | 151.35 ± 4.42 | 219.41 ± 7.94 |
| C.R. | 0.70 ± 0.01 | 0.54 ± 0.01 |

Table 1: Quantitative description of C2C12 cell morphology under different hypertonic stress. Area (µm²), perimeter (µm), Ctrl=Control group.

3.4.3 Cell migration on a gradient-compliant PA gel

The windrose plots (Fig 3.10) qualitatively show C2C12 cells migration path on a gradient-compliant PA gel. We divide the cell tracking points into two categories, one is harder region (hard in Fig 3.10) where the elasticity of the substrate is large than 12 kPa, and the other is softer region (mid and soft in Fig 3.10) where the elasticity of the substrate is small than 12 kPa. The preferred migration directions of C2C12 cells are opposite in the two regions. However, the quantitative analysis (Fig 3.11) shows only C2C12 cells from the hard region have a significant TI value compared to zero (no biased). The mean of TI in hard region is 0.22 (table 2) which represents a strong biased migration driven by stiffness gradient (Isenberg, DiMilla et al. 2009; Sochol, Higa et al. 2011). The cell migration difference is similar with previous studies, which demonstrated that cell migration speed is faster on a softer substrate (Lo, Wang et al. 2000; Wong, Velasco et al. 2003).

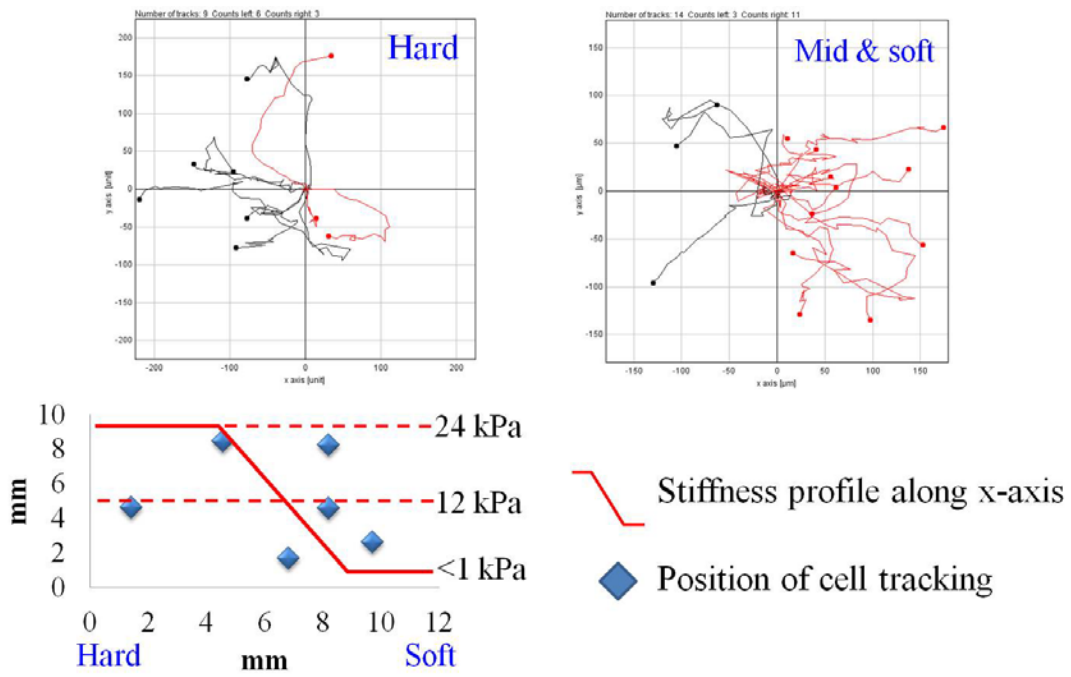


Fig. 3.10: Windrose plot of cell migration path and positions of cell tracking on a gradient-compliant PA gel.

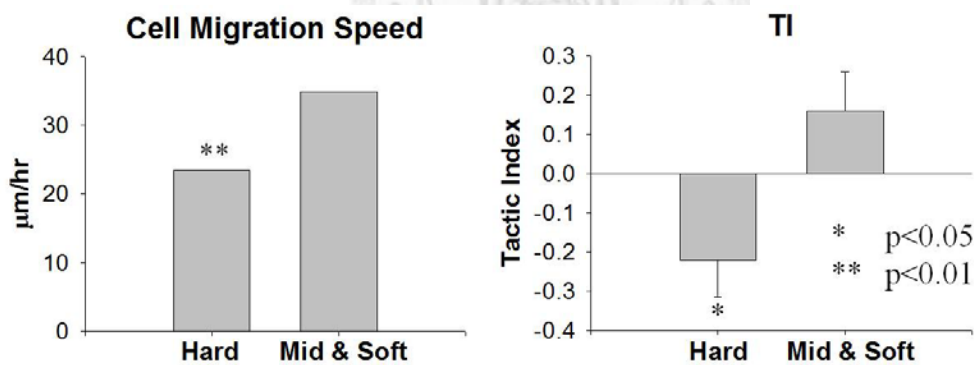


Fig. 3.11: Quantitative analysis of C2C12 cell migration speed and TI.

| Cell migration analysis (Mean ± SEM) | | |
|--------------------------------------|---------------|--------------|
| | Speed (μm/hr) | TI |
| Hard (n=9) | 23.4 ± 0.03 | -0.22 ± 0.09 |
| Mid & Soft (n=14) | 34.8 ± 0.05 | 0.16 ± 0.10 |

Table 2: Quantitative description of C2C12 cell migration speed and TI.

The cell number distribution among different position is shown in fig 3.10. This data showed a trend that the cell would accumulate at harder region. Consider the average migration speed of C2C12 cells is about $30\mu\text{m/hr}$ (Table 1), the trend might be more significant if we culture the cells for more days (*e.g.* one week). The distribution is also important to evaluate whether the C2C12 cell can respond to stiffness gradient.

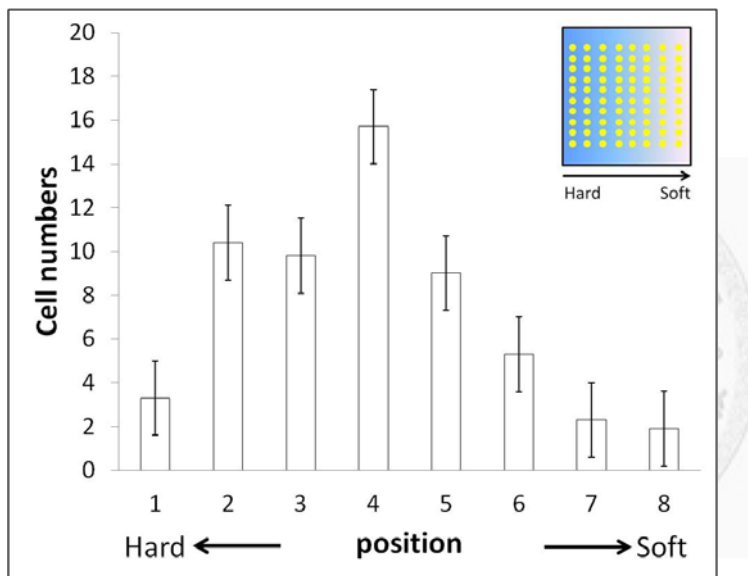


Fig. 3.12: Distribution of cell numbers along a gradient-compliant PA gel.

The gel was equally separated into eight columns, and each column was further separated into ten rows. Therefore, there are ten data points in each column. The number in the x-axis represents each column sequentially from the hard region to the soft region. The cell numbers were described in Mean \pm SEM of the ten data points in each column.

3.5 Evaluation of 2D and 3D hydrogel-microfluidic integration systems

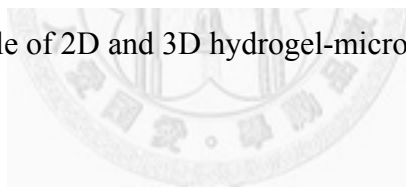
Besides embedding a 2D gel in a microfluidic system, fabricating a 3D gel in the microfluidic channels would be another design strategy, such as the device developed by Kamm's group (Chung, Sudo et al. 2009; Chung, Sudo et al. 2010). In brief, the prepolymer solution can fill in specific channels and polymerize to form a 3D scaffold. This would be easy and intuitive to embed a hydrogel in the microfluidic system. However, the micro-pillar structure design (to confine gel in a specific region) or a customized micro-injection tool would increase the fabrication complexity. The main advantage of Kamm's device would be a 3D cell culture environment and co-culture. Despite the co-culture can not be operated in the single cell level, the interaction between two groups of cell can still provide insightful information to cell behavior research.

Two important issues to this device would be stiffness control and cell tracking technique. For most materials used in 3D structure, such as collagen, the biomechanical cues are coupled to some biochemical cues. If the polymerized degree of collagen gel were changed, the porosity or pore size of the gel would also be different. Therefore, the cell would also sense different density of the ECM protein besides stiffness difference. For cell tracking, it can not be performed as easy as in 2D surface. Sometimes the cell has to carry fluorescent protein for live image tracking.

The total distance of cell migration is also hard to measure, thus a projected length is used in most cases. Although we only take two examples to compare (table 3), the strengths and weaknesses listed should be appropriate to represent general cases.

| Cell culture substrate | 2D | 3D |
|-----------------------------------|-------------------------------------|---------------------------|
| Example | Our lab | Kamm's group |
| Hydrogel | Polyacrylamide | Collagen |
| Fabrication complexity | Middle | Middle |
| Cell tracking and analysis | Good | Middle |
| Stiffness gradient | Yes | No |
| Chemical gradient | Yes | Yes |
| Co-culture | No | Yes (limited) |
| Main advantage | Stiffness gradient Cell tracking | 3D scaffold Co-culture |

Table 3: A comparison table of 2D and 3D hydrogel-microfluidic integrated systems.



Chapter 4. Conclusion and Future works

We have successfully developed a unique fabrication process to integrate a gradient-compliant PA gel into a microfluidic system. Most of the characteristics of the gradient-compliant PA gel have been evaluated. The ability to generate concentration gradients through our device has also been demonstrated. In theory, this integrated PA gel-microfluidics device could generate two well-controlled mechanical cues simultaneously to guide cell migration. The C2C12 cell experiments also provide important information for further experimental design to test our hypotheses.

To fully demonstrate the potential of our device, there are three important future works. First of all, establish a protocol or a solid approach to well control the inlet flow. It is especially important since we need the flow to be slow enough such that the movement of solutes will be similar with random walk. Passive pump or osmotic pump (Park, Hwang et al. 2007) are possible solutions and good references to control very slow speed flow. The challenge would be learning about these two approaches.

Secondly, eliminate the structure defects. These defects will interfere with the control to the concentration gradients, thus increasing the complexity of quantifying the relationship between signals and cell migration. Besides the lock and key design described before, fabricate the master mold of PDMS substrate through

photolithography will also be useful. The difficulty would be familiar with multi-layer SU-8 photoresist processing to construct the spacing in fig 2.7. Another good approach is to fabricate thin-film PDMS substrate (Jo, Van Lerberghe et al. 2000). Besides eliminating structure defects, we can replace the groove with a hole, thus removing the cost of customized Glass_1. It may also enable our device be capable to be studied with high power objective lens. The difficulty would be establishing an effective protocol to reproduce the thin-film PDMS substrate.

Finally, use other cell types to evaluate the performance of our device. For example, VSMC cells, which has been shown that they would respond to stiffness gradient. Another example, the astrocyte, which has been demonstrated that it prefers to migrate to the hypotonic region. Although it may increase the cost of the reagents for cell culture, we can benefit from shortening the time to confirm our device function well. That will certainly accelerate the optimization of this dual cues device.

For C2C12 cell migration studies, we can evaluate TI value to verify the impacts of stiffness and osmotic gradients on guiding cell migration. The migration speed difference between single cue and dual cues (e.g. osmotic and stiffness gradients in parallel) would be an appropriate approach to test the facilitation between the two signals.

Reference

Alfieri, R. R., M. A. Bonelli, et al. (2006). "Creatine as a compatible osmolyte in muscle cells exposed to hypertonic stress." The Journal of physiology **576**(2): 391-401.

Barkefors, I., S. Le Jan, et al. (2008). "Endothelial cell migration in stable gradients of vascular endothelial growth factor A and fibroblast growth factor 2." Journal of Biological Chemistry **283**(20): 13905-13912.

Chung, S., R. Sudo, et al. (2009). "Cell migration into scaffolds under co-culture conditions in a microfluidic platform." Lab Chip **9**(2): 269-275.

Chung, S., R. Sudo, et al. (2010). "Microfluidic platforms for studies of angiogenesis, cell migration, and cell–cell interactions." Annals of biomedical engineering **38**(3): 1164-1177.

Engler, A. J., M. A. Griffin, et al. (2004). "Myotubes differentiate optimally on substrates with tissue-like stiffness." The Journal of cell biology **166**(6): 877-887.

Engler, A. J., F. Rehfeldt, et al. (2007). "Microtissue elasticity: measurements by atomic force microscopy and its influence on cell differentiation." Methods in cell biology **83**: 521-545.

Engler, A. J., S. Sen, et al. (2006). "Matrix elasticity directs stem cell lineage specification." Cell **126**(4): 677-689.

Gardel, M. L., I. C. Schneider, et al. (2010). "Mechanical integration of actin and adhesion dynamics in cell migration." Annual review of cell and developmental biology **26**: 315-333.

Grattoni, C. A., H. H. Al-Sharji, et al. (2001). "Rheology and permeability of crosslinked polyacrylamide gel." Journal of colloid and interface science **240**(2): 601-607.

Gribova, V., T. Crouzier, et al. (2011). "A material's point of view on recent developments of polymeric biomaterials: control of mechanical and biochemical

properties." J. Mater. Chem. **21**(38): 14354-14366.

Hanson, L., L. Cui, et al. (2011). "A microfluidic positioning chamber for long-term live-cell imaging." Microscopy Research and Technique **74**(6): 496-501.

Hwang, S. M., R. H. Lee, et al. (2002). "Expression of aquaporin-5 and its regulation in skeletal muscle cells." Experimental & molecular medicine **34**(1): 69.

Isenberg, B. C., P. A. DiMilla, et al. (2009). "Vascular smooth muscle cell durotaxis depends on substrate stiffness gradient strength." Biophysical journal **97**(5): 1313-1322.

Jaeger, M., M. Carin, et al. (1999). "The osmotic migration of cells in a solute gradient." Biophysical journal **77**(3): 1257-1267.

Jo, B. H., L. M. Van Lerberghe, et al. (2000). "Three-dimensional micro-channel fabrication in polydimethylsiloxane (PDMS) elastomer." Microelectromechanical Systems, Journal of **9**(1): 76-81.

Kadow, C. E., P. C. Georges, et al. (2007). "Polyacrylamide hydrogels for cell mechanics: steps toward optimization and alternative uses." Methods in cell biology **83**: 29-46.

Li Jeon, N., H. Baskaran, et al. (2002). "Neutrophil chemotaxis in linear and complex gradients of interleukin-8 formed in a microfabricated device." Nature biotechnology **20**(8): 826-830.

Lo, C. M., H. B. Wang, et al. (2000). "Cell movement is guided by the rigidity of the substrate." Biophysical journal **79**(1): 144-152.

Loitto, V. M., T. Karlsson, et al. (2009). "Water flux in cell motility: expanding the mechanisms of membrane protrusion." Cell motility and the cytoskeleton **66**(5): 237-247.

Nemir, S., H. N. Hayenga, et al. (2010). "PEGDA hydrogels with patterned elasticity: Novel tools for the study of cell response to substrate rigidity." Biotechnology and bioengineering **105**(3): 636-644.

- Papadopoulos, M., S. Saadoun, et al. (2008). "Aquaporins and cell migration." Pflügers Archiv European Journal of Physiology **456**(4): 693-700.
- Park, J. Y., C. M. Hwang, et al. (2007). "Gradient generation by an osmotic pump and the behavior of human mesenchymal stem cells under the fetal bovine serum concentration gradient." Lab Chip **7**(12): 1673-1680.
- Park, J. Y., S. J. Yoo, et al. (2009). "Simultaneous generation of chemical concentration and mechanical shear stress gradients using microfluidic osmotic flow comparable to interstitial flow." Lab Chip **9**(15): 2194-2202.
- Saadoun, S., M. C. Papadopoulos, et al. (2005). "Involvement of aquaporin-4 in astroglial cell migration and glial scar formation." Journal of cell science **118**(24): 5691-5698.
- Sochol, R. D., A. T. Higa, et al. (2011). "Unidirectional mechanical cellular stimuli via micropost array gradients." Soft Matter.
- Tse, J. R. and A. J. Engler (2010). "Preparation of hydrogel substrates with tunable mechanical properties." Curr Prot Cell Bio Chpt **10**: 1-16.
- Van Donkelaar, C., M. Daniels, et al. (2003). "Cell deformation in response to long-term hyperosmotic loading." Acta of Bioengineering and Biomechanics **5**(1): 3-10.
- Wong, J. Y., A. Velasco, et al. (2003). "Directed movement of vascular smooth muscle cells on gradient-compliant hydrogels." Langmuir **19**(5): 1908-1913.